Electronic Supplementary Material (ESI) for ChemComm.

Electronic Supplementary Information

for

An *in-situ* assembly strategy for construction of sensitive and reusable electrochemical aptasensor

Juan Song[a], Songling Li[a], Feng Gao[a], Qingxiang Wang[a,*], Zhenyu Lin[b,*]

a. College of Chemistry and Environment, Fujian Provincial Key Laboratory of Modern Analytical Science and Separation Technology, Minnan Normal University, Zhangzhou, 363000, China. E-mail: axiang236@126.com

b. MOE Key Laboratory of Analysis and Detection for Food Safety, Fujian Provincial Key Laboratory of Analysis and Detection Technology for Food Safety, Institute of Nanomedicine and Nanobiosensing, College of Chemistry, Fuzhou University, Fuzhou, 350116, China. Email: zylin@fzu.edu.cn

Table of contents

1. Experimental Section

Reagents. Potassium chloride (KCl), hydrochloric acid (HCl), sodium hydroxide (NaOH), potassium ferricyanide ($K_3Fe(CN)_6$), potassium ferrocyanide ($K_4Fe(CN)_6$), sulfuric acid (H_2SO_4), hydrogen peroxide (H_2O_2), magnesium chloride ($MgCl_2$), sodium chloride (NaCl), copper nitrate ($Cu(NO_3)_2$), ethylenediaminetetraacetic acid (EDTA) were obtained from Guangdong Xilong Chemical Co., Ltd. (China); *L*-cysteine (*L*-cys), sodium 3-morpholinopropanesulfonatebsodium salt (MOPs) and tris (hydroxymethyl) aminomethane (Tris) were provided by Aladdin Reagent Co., Ltd. (China). Tris (2-carboxyethyl) phosphine hydrochloride (TCEP), 6-mercapto-1-hexanol (MCH), thrombin, bovine serum albumin (BSA), hemoglobin (Hb) and lysozyme (Lyso) were purchased from Sigma-Aldrich reagent Co., Ltd. (China). Chloroauric acid ($HAuCl_4 \cdot 4H_2O$) was obtained from Sinopharm Chemical Reagent Co., Ltd. (China). Sodium borohydride ($NaBH_4$) and cetyltrimethylammonium bromide (CTAB) were purchased from Alfa Aeasar Co., Ltd. (England). All aqueous solutions were prepared in ultrapure water, which was obtained from a Milli-Q water purifying system (18 MΩ▪cm). All the chemicals were of analytical grade and used without further purification.

Thiolated supporting sequence (TSS) (5′-SH-$(CH_2)_6$-GGG CCA ACC ACA-3′) and thiolated thrombin aptamers (TBA) (5′-SH-$(CH_2)_6$-GGT TGG TGT GGT TGG-3′) were purchased from Sangon Biotech Co., Ltd. (Shanghai, China). Both of the two sequences and thrombin were prepared with mixed Tris buffer solution containing 100 mM NaCl, 100 mM $MgCl_2$, 10 mM TCEP, 25 mM Tris-HCl and kept at 4 ℃ for further use. The prepared DNA electrode was washed with MOPs buffer (pH 8.0) with 20 mM NaCl, 20 mM $MgCl_2$. Supporting electrolyte for electrochemical measurements (pH 8.0) was 0.1 M H_3BO_3 containing 0.1 M KCl and 2.5 % (V/V) ethanol.

Apparatus. An electrochemical workstation in connection with CHI 650D, a conventional China three-electrode system was used for analysis. The bare or modified gold electrode (AuE) as working electrode, a platinum wire as auxiliary electrode and an Ag/AgCl (3 M KCl) as reference electrode. Atomic force microscopy (AFM) images was utilized for morphology characterization of the electrode, which was carried on a CSPM 5500 scanning probe microscope (China).

2. Synthesis of AuNPs and electrode pre-treatment

AuNPs were prepared according to a previously reported [1]. Briefly, CTAB-capped Au seeds were synthesized by chemical reduction of $HAuCl_4$ with $NaBH_4$: CTAB (7.5 mL, 0.1 M) was mixed with $HAuCl_4$ (100 μL, 25 mM) and diluted with water to 9.4 mL. Then, the ice-cold $NaBH_4$ (0.6 mL, 0.01 M) was added under magnetic stirring. The solution color turned immediately from bright yellow to brown, indicating formation of the gold seeds. Then the mixture was purified by centrifuging at 10000 rpm for 5 min, and precipitate was collected and finally re-dispersed in ultrapure water.

Prior to experiment, the AuE was carefully polished successively with 1.0, 0.3, and 0.05 μm alumina powder to obtain a mirror electrode surface. Then, the electrode was sonicated in ultrapure water, mixture of water and ethanol (V_{water}: $V_{ethanol}$ = 1:1) and ultrapure water for 5 min, respectively, to remove the residual Al_2O_3 power. Subsequently, the cleaned electrode was activated in Piranha solution ($V_{30\%H2O2}$:$V_{98\%H2SO4}$=7:3) for 20 min. Followed by, the electrodes were scanned in 0.5 M H_2SO_4 from -0.2 to 1.6 V at 100 mV s^{-1} until steady curves were achieved. Afterward, the AuE was washed thoroughly with ultrapure water and dried by nitrogen.

3. Fabrication of the biosensing interface

First, the TSS modified AuE (TSS/AuE) was prepared by immersing the cleaned electrode into 0.1 μM TSS solution for 24 h at 4 °C, through which the TSS was confined on the gold electrode through Au-S bond. Then, the sensor was treated with 1 mM MCH for 2 h to passivate the unmodified region of electrode, and the obtained electrode was denoted as TSS/MCH/AuE. The hybridization of TSS with partial complementary aptamer sequence TBA was performed by incubating the TSS/MCH/AuE in 1.0 mM TBA solution for 50 min under room temperature. Then the electrode was washed with MOPs to remove the non-specifically adsorbed TBA, and the hybridized electrode TBA-TSS/MCH/AuE was achieved. What's more, the electrode was immersed into AuNPs solution for 3 h to assemble AuNPs on 5'-end of TBA, and the prepared electrode was termed as AuNPs/TBA-TSS/MCH/AuE. Immediately, the *L*-cys was immobilized on AuNPs/TBA-TSS/MCH/AuE through incubating the electrode in 1 mM *L*-cys. Followed by, the electrode was washed with ultrapure water to remove the non-specifically *L*-cys to get the *L*-cys/AuNPs/TBA-TSS/MCH/AuE. Finally, the modified electrode was dipped into 5 mM $Cu(NO_3)_2$ solution for 30 min at 37 °C and then immersed into the mixture of 10 mM MOPs

buffer (pH 8.0) with 20 mM NaCl and 20 mM $MgCl_2$ for 30 min to remove physically bound Cu^{2+}. Thus, the Cu^{2+} labeled sensing interface was prepared, which was denoted by Cu^{2+}-*L*-cys/AuNPs/TBA-TSS/MCH/AuE.

4. Thrombin binding and electrochemical measurements

The hybridization reaction of the developed biosensor was investigated by incubating Cu^{2+}-*L*-cys/AuNPs/TBA-TSS/MCH/AuE into a hybridization buffer containing target thrombin with desired concentrations for 30 min under 37 ^{o}C with gentle shaking. After rinsing with MOPs buffer, the hybridized electrode was fabricated. The procedure was also applied for the hybridization of the biosensor with the other proteins.

The electrochemical characterization was carried out in 1.0 mM $[Fe(CN)_6]^{3-/4-}$ solution containing 0.1 M KCl via cyclic voltammetry (CV) and electrochemical impendence spectra (EIS). The scan range of CV from -0.2 to +0.6 V with the scan rate of 100 mV s^{-1}. The EIS was collected at a potential of +0.197 V in the frequency range of 10^5~1 Hz with the voltage amplitude of 5 mV. The electrochemical behavior of the biosensor and its recognition to thrombin detection were obtained from CV and differential pulse voltammetry (DPV) in the mixture of 0.10 M H_3BO_3 (pH 8.0), 0.1 M KCl and 2.5% (V/V) ethanol. The response was recorded within the potential range from -0.2 V to +0.6V.

5. Construction idea and working principle of the sensor

The construction idea of the sensing interface and its working mechanism for the detection of thrombin are as follows. First, TSS strands were immobilized onto the surface of gold electrode by strong Au-S bond. Then the MCH molecule was assembled on electrode to form the ordered layer with TBA by occupying residue site of AuE. Afterword, the recognition strand of TBA was hybridized with strands, and AuNPs and *L*-cys were grafted onto the 5'-thiolated TSS in turn through Au-S bonds. Finally, the source Cu^{2+} was coordinated with -NH_2 and -COOH of *L*-cys to achieved the electro-active biosensing interface. When the target thrombin was presented in solution to competitively interact with TBA strands, the TBA with the *in-situ* grafted AuNPs/*L*-cys/Cu^{2+} departures from the electrode surface, causing attenuation of the electrochemical response of the fabricated biosensor. Through such a strategy, the thrombin biosensor can be

simply prepared, and the concentration of thrombin can be well detected by monitoring the signal attenuation of the biosensor. It is noticeable that the competitive binding a widely used method for bioanalysis, but compared with traditional methods, the competitive binding strategy developed in this work has its own advantage, namely, the assistant strands of TSS is confined on the electrode surface, and then the TBA is attached on electrode surface via hybridization with TSS. Thus, when the target molecule of thrombin is interacted with TBA, the complex will fall off from the electrode surface, enabling the TSS electrode being reusable.

6. Electrochemical characterization on the fabrication of the sensor

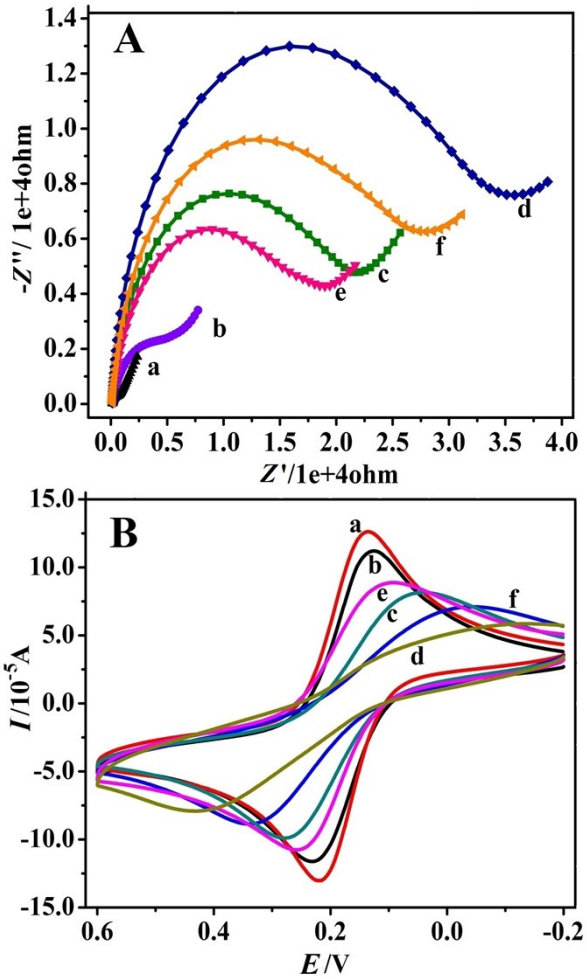

Fig. S1 EIS (A) and CV (B) of bare AuE (a), TSS/AuE (b), TSS/MCH/AuE (c), TBA-TSS/MCH/AuE (d), AuNPs/TBA-TSS/MCH/AuE (e) and *L*-cys/AuNPs/TBA-TSS/MCH/AuE (f) in 1 mM $[Fe(CN)_6]^{3-/4-}$ solution containing 0.1 M KCl with scan rate of 100 mV s^{-1}.

The stepwise fabrication process of the sensor was electrochemically characterized using $[Fe(CN)_6]^{3-/4-}$ as the redox probe, and the EIS and CV results are showed in Fig. S1 (A) and Fig.

S1 (B), respectively. In EIS, the electron transfer resistance (R_{ct}) is directly estimated from the semicircle diameter at the high frequency region [2]. A linear part is obtained on bare AuE (curve a), which shows that the electrochemical response of $[Fe(CN)_6]^{3-/4-}$ on the bare AuE is mainly controlled by a diffusion procedure. After TSS has been immobilized onto the AuE, the electrode obtains a significant increase in the nyquist plots (Fig. S1 (A)) and the R_{ct} values of 7.5 kΩ (curve b) is recorded, which is due to the electrostatic repulsion between $[Fe(CN)_6]^{3-/4-}$ and DNA. When the TSS/AuE has been modified with MCH, the unoccupied part of the AuE is further blocked and the R_{ct} value is raised to 25 kΩ (curve c). After the electrode was immersed in the TBA for hybridization, the DNA duplex was formed, leading to the kinetics barrier between $[Fe(CN)_6]^{3-/4-}$ and negatively charged phosphate backbones, and so the EIS response was dramatically increased to 40 kΩ (curve d). When the electrode was modified with AuNPs, the R_{ct} was markedly decreased to 22 kΩ (curve e) due to the good electrical conductivity of AuNPs, which also suggested that AuNPs has been successfully assembled on the surface of electrode. Then the modified electrode was immersed into *L*-cys solution, which would graft onto the surface of AuNPs through the strong Au-S bond. As a result, R_{ct} of the electrode significantly increased to 32.5 kΩ again (curve f). This could be explained by the coating of AuNPs by the non-conductive *L*-cys layer and weaken the electron transfer promotion capacity of AuNPs.

Fig. S1B shows the corresponding CV of different electrodes in mixture of $[Fe(CN)_6]^{3-/4-}$ and KCl within potential range from -0.2 V to 0.6 V. It is obviously observed that a couple of well-defined reversible redox peaks at 141 mV and 225 mV [3, 4], suggesting good electron transfer of $[Fe(CN)_6]^{3-/4-}$ at bare AuE (curve a). The potential difference of the two peaks was 84 mV, and the peak current ratio ($|I_{pa}/I_{pc}|$) was close to 1, certifying that the AuE has been well cleaned and act as a good electron transfer conductor. However, when the AuE was modified with the TSS through Au-S bond, the redox peak currents of $[Fe(CN)_6]^{3-/4-}$ decreased remarkably and the redox potential difference was enlarged obviously (curve b), which could be explained in term of the electrostatic repulsion between $[Fe(CN)_6]^{3-/4-}$ and TSS. After the electrode was modified with MCH, the peak currents of $[Fe(CN)_6]^{3-/4-}$ further decrease as (curve c). When the TBA was modified on the electrode, the peak current decreased again (curve d), which could be ascribed to increase of electrostatic repulsion force and steric hindrance effect of electrode surface to $[Fe(CN)_6]^{3-/4-}$. Then when AuNPs were grafted to the end of TBA, the high conductivity of AuNPs promoted the

electronic transfer, causing obvious increase of redox signal. When the electrode assembly with *L*-cys, the current was deceased significantly and the potential difference of the two peaks was increased, confirming the *L*-cys molecules had been anchored on AuNPs and covered the active site of AuNPs surface. All experimental results demonstrated that the sensing interface had been successfully fabricated.

7. Optimization of experimental conditions

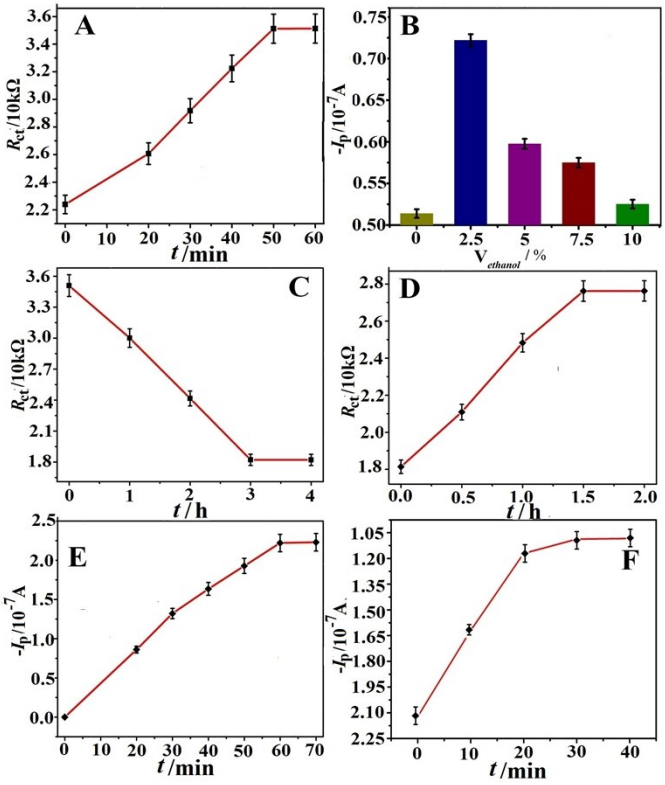

Fig. S2 Relationship of R_{ct} values versus hybridization time of TSS/MCH/AuE with 100 pM TBA (*t*) (A). Effect of content (V/V) of ethanol in the test electrolyte (B). Dependence of the incubating time of AuNPs (C), *L*-cys (D) and Cu^{2+} (E). Influence of the reaction time of thrombin on the experiment (F); (all the I_p were DPV peak current, and the R_{ct} were measured from EIS).

In order to achieve the highest performance of the sensor, some experimental conditions such as the hybridization time of TSS with TBA, ethanol content (V/V) in the electrolyte, the incubating time of AuNPs, the assembly time of *L*-cys and Cu^{2+} for physically absorbed and the reaction time of thrombin are optimized. Fig. S2 (A) shows the relationship of R_{ct} value of the electrode in $[Fe(CN)_6]^{3-/4-}$ versus the hybridization time. It can be clearly seen that the R_{ct} increased significantly from 0 min to 50 min, which indicts increasing number of TSS has been

hybridized with TBA. When the hybridization time reaches 50 min, the R_{ct} value changes hardly, suggesting that the TSS has been reacted completely with TBA. So we choose 50 min as the optimal hybridization reaction time between TSS and TBA. It has been reported that the presence of certain amount of ethanol in the test electrolyte can effectively improve the stability and electrochemical intensity of the copper complex [5]. Therefore, in this work, the influence of the ethanol on the electrochemical biosensor is also investigated (Fig. S2A), it is found that when the content of ethanol changes from 0 to 10 % (V/V), the largest electrochemical signal is achieved for the sensor at 2.5% (V/V). Hence, the solution of 0.1 M H_3BO_3 (pH 8.0) containing 0.1 M KCl with 2.5% (V/V) ethanol is chosen as the supporting electrolyte. The incubating time of AuNPs (C) are also investigated. As seen from the Fig. S2 that the R_{ct} is tended to be unchanged at 3 h, indicating the modified electrode surface has reached to saturation. Therefore, 3 h is chosen as the incubation time of AuNPs. Fig. S2 (D) shows the effect reaction time of *L*-cys of on oxidation peak currents (I_{pa}) of the biosensor, it is clearly that when the accumulate time reached at 1.5 h, the response is almost unchanged, therefore, 1.5 h is chosen as the optimal reaction time between AuNPs and *L*-cys. Fig. S2E shows the relationship between DPV peak current (I_p) and incubation time of *L*-cys/AuNPs/TBA-TSS/MCH/AuE in Cu^{2+} solutions. Obviously, the electrochemical signal increases with the prolong the incubation time, the peak currents increases clearly and tended to level off when the time reaches to 60 min, which is an indicator of the coordination saturation of Cu^{2+} with *L*-cys. Fig. S2(F) depicts effect of the reaction time of thrombin with TBA on the electrode surface. With increase of binding time of TBA and thrombin, the electrochemical signal is dropped, and when the time reaches 30 min, the currents decreases to steady, which indicates a binding saturation of thrombin with TBA on the sensor. Thus, 30 min is chosen as the optimal reaction time of thrombin.

8. Stability of the aptasensor

Furthermore, the stability of the biosensor also detected by keeping the well modified electrode in the fridge at 4 °C for 5 weeks. It found that only 6.47% loss in the current signal was observed, showing a good stability of the biosensor.

Table S1. Comparison of the proposed biosensor with other TBA-based electrochemical thrombin biosensors

Biosensors	Linear range	Detection limit	Refs.
Fc-DNA/MCH/MB-DNA/DWs/TBA/AuNPs/GCE	0.1 pM-10 pM	56 fM	6
TBA/GO/GCE	0.1 nM -10 nM	70 pM.	7
MB-P3-AuNPs/TBA/MCH/Fc-HP/AuE	3 pM-30 nM	1.1 pM	8
TBA/PDA/AgNPs/GCE	0.1 pM -5.0 nM	36 fM	9
TBA/ HBPE-SO_3/Au/MPTMS/GCE	2.70 pM - 270 nM and 1.35 μM-27.0 μM	31 fM	10
Cu_2O-AuNPs-BSA/NH_2-TBA/AuNPs/GCE	100 fM to 20 nM	23 fM	11
pTBA/Apt/ MNP@Ab-TBO/ SPCEs	1.0 nM to 500 nM	49 pM	12
Cu^{2+}-*L*-cys/AuNPs/TBA-TSS/MCH/AuE	100 fM -2.0 μM	21 fM	This work

Note: Fc: ferrocene; MB: methylene blue; TBA: thrombin aptamer; DWs: DNA walkers; AuNPs: gold nanoparticles; GO: graphene oxide; HP: Heparin; P3: bio-bar-coded; AuE: gold electrode; AgNPs: sliver nanoparticles; GCE: glassy carbon electrode; PDA: polydopamine. HBPE: hyperbranched polyester; MPTMS: 3-mercaptopropyltrimethoxysilane; pTBA: (poly-2,2′,5′,5″-terthiophene-3′-p-benzoic acid; MNP: magnetic nanoparticle; Ab: thrombin antibodies; TBO: toluidine blue O; SPCEs: screen-printed carbon electrodes.

Table S2. Determination of thrombin in serum samples using the developed aptasensor[a]

Sample	Amount spiked /nM	Amount measured[a] /nM	Recovery/ %
1	0.025	0.024	96.0%
2	0.10	0.103	103%
3	5.0	5.12	102%
4	50	48.5	97.0%

[a] Mean values of three measurements.

References

1. M. J. A. Shiddiky, M. A. Rahman and Y. B. Shim, *Anal. Chem.* 2007, **79**, 6886-6890.
2. C. X. Zhu, M. Y. Liu, X. Y. Li, X. H. Zhang and J. H. Chen, *Chem. Commun.,* 2018, **54**, 10359-10362.
3. K. J. Babu, S Sheet, Y. S. Lee and G. G. kumar, *ACS Sustainable Chem. Eng.,* 2018, **6**, 1909-1918.
4. F. P. Zhan, X. L. Liao, F. Gao, W. W. Qiu and Q. X. Wang, *Biosens. Bioelectron.,* 2017, **92**, 589-595.
5. C. D. Brondino and R. Calvo, *Inorg. Chem.,* 1997, **36**, 3183-3187.
6. C. X. Zhu, M. Y. Liu, X. Y. Li, X. H. Zhang and J. H. Chen, *Chem. Commun.,* 2018, **54**, 10359-10362.
7. F. AhourM and K. Ahsani, *Biosens. Bioelectron.,* 2016, **86**: 764-769.
8. L. L. Wang, R. N. Ma, L. S. Jiang, L. P. Jia, W. L. Jia and H. S. Wang, *Biosens. Bioelectron.* 2017, **92**, 390-395.
9. Q. J. Xu, G. X. Wang, M. M. Zhang, G. Y. Xu, J. H. Lin and X. L. Luo, *Microchim. Acta,* 2018, **185**, 253.
10 Y. L. Niu, M. L. Chu, P. Xu, S. S. Meng, Q. Zhou, W. B. Zhao, B. Zhao and J. Shen, *Biosens. Bioelectron.,* 2018, **101,** 174-180.
11 S. Chen, P. Liu, K. W. Su, X. Li, Z. Qin, W. Xu, J. Chen, C. R. Li and J. F. Qiu*, Biosens. Bioelectron.,* 2018, **99,** 338-345.
12 S. Chung, J. M. Moon, J. Choi, H. Hwang and Y. B. Shim, *Biosens. Bioelectron.,* 2018, **117**, 480-486.